Simulation of Buckled Cantilever Plate with Thermal Bimorph Actuators

Arpys Arevalo*[1], David Conchouso[1], David Castro[1], Marlon Diaz[2], Yi Ying[3], and Ian G. Foulds[1,3]
[1]Computer, Electrical and Mathematical Sciences and Engineering (CEMSE), King Abdullah University of Science and Technology (KAUST), [2]Physical Sciences and Engineering (PSE), King Abdullah University of Science and Technology (KAUST), [3]The University of British Columbia (UBC), School of Engineering, Okanagan Campus.
*Corresponding author: 4700 KAUST, Kingdom of Saudi Arabia, arpys.arevalo@kaust.edu.sa

Abstract: In this paper we simulated a Buckled Cantilever Plate (BCP) with thermal bimorph micro-actuators that allows the manipulation of out-of-plane structures through the adjustment of the pitch angle. Two physics were used in the simulation, first the Structural Mechanics for the assembly of the out-of-plane structure and secondly the a Heat Transfer simulation using the Joule Heating Module in order to visualize the deformation and displacement of the plates under operation. Experimental results have shown displacements larger than $300\mu m$. The accurate control of the angular position that is possible using this mechanism, makes them suitable candidates for a range of different MEMS applications, such as: optical benches, low frequency sweeping sensors and antennas.

Keywords: MEMS, Bimorph Actuator, Buckled Cantilever, Polyimide.

1. Introduction

Micro Electro Mechanical Systems (MEMS) are fabricated with an in-plane fabrication technology. Out-of-plane structures can be designed to be assembled to provide thermal and electrical isolation from the substrate [1–3]. These isolations can potentially improve the performance of a range of MEMS devices by decreasing any unwanted coupling effects or parasitic loses from the fabricated devices, to a lossy substrate. One of the interesting out-of-plane mechanism is the Buckled Cantilever Plate (BCP) [3–5] and the other one is the Tsang Suspension [6, 7]. We have designed and simulated BCP out-of-plane structures with thermal bimorph actuators to be able to control the angular position of the assembled plate Fig. 1.

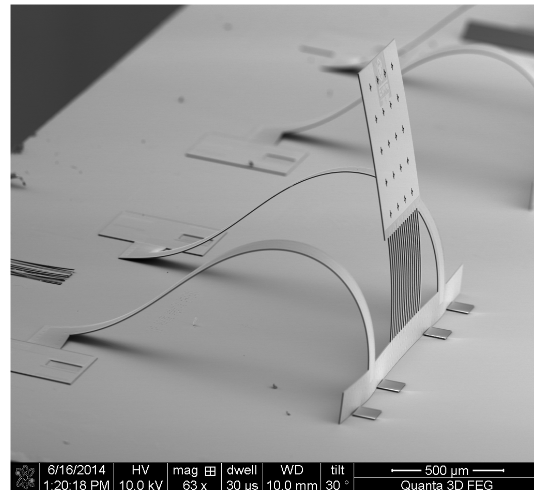

Figure 1: Scanning Electron Microscope (SEM) image of an assembled BCP structure with thermal bimorph actuators.

The BCP structures are compliant mechanisms that when deformed make use of their material's elastic properties, to maintain a position using stoppers and its reaction forces.

There have been a few applications demonstrated using BCP structures. For example, radio frequency antennas with greater performance efficiency due to the separation from the lossy silicon substrate [8]. Others, have tried micro-heater for gas sensing applications [9], thermal accelerometers [10] and magenetic field induction sensors [11].

Our device has an integrated set of thermal bimorph actuators, which enables a precise dynamic tuning of the structural plate angular position. A bimorph thermal actuator is composed typically by a bilayer structure, two materials with different

coefficient of thermal expansion. The structural layer of the device is polyimide. The polymer has demonstrated good mechanical performance for MEMS devices, in comparison to other materias such as SU-8 [12–14] and silicon used as the structural material in and also flexible electronics [15, 16], appropriate for MEMS devices [3, 17–24] Material properties such as a low thermal expansion coefficient, operation temperature of up to $350^{\circ}C$ and good chemical stability, allows its usage in a wide variety of applications. The structures design will be discussed in the design section.

2. Computational Methods

The Solid Mechanics interface solves the equations of motion together with a constitutive model for a solid material. From these solutions, COMSOL can compute results on the structure displacements, strains and stresses [25]. The MEMS and Structural Mechanic modules provide several features, like geometric nonlinearity and advanced boundary conditions such as contact, follower loads, and nonreflecting boundaries [25].

2.1 Governing Equations

The analysis of deformation describes the local deformation in a material suitable for use in a constitutive relation, which frequently derives to a strain tensor.

The formulation used for structural analysis in COMSOL Multiphysics for bot small and finite deformation is a Total Lagrangian formulation. Which means, that the computed stress and deformation state is referred to as the material configuration and not to the current position in space [25].

Consider a certain physical particle, with an initial position at the coordinate $\mathbf{X}$. When the particle is deformed, it follows a path

$$\mathbf{x} = \mathbf{x}(\mathbf{X}, t) \tag{1}$$

where, $\mathbf{x}$ is the spatial coordinate and $\mathbf{X}$ is the material coordinate.

To simplify, COMSOL assumes that undeformed and deformed position are measured in the same coordinate system [25]. It uses the displacement $\mathbf{u}$ in order to be possible to use the following equation

$$\mathbf{x} = \mathbf{X} + \mathbf{u}(\mathbf{X}, t) \tag{2}$$

The displacement is a function of the material coordinates (X, Y, Z), without being an explicit function of the spatial coordinates (x, y, z). Therefore, it is only possible to compute derivatives with respect to the material coordinates [25].

In the following equation (3), the gradient operator is to be assumed as a gradient with respect to the material coordinates, unless it is stated different.

$$\nabla = \nabla_X = \left[\frac{\delta}{\delta X} \frac{\delta}{\delta Y} \frac{\delta}{\delta Z} \right] \tag{3}$$

The gradient of the displacement is always computed with respect to the material coordinates. In 3D:

$$\nabla \mathbf{u} = \begin{bmatrix} \frac{\delta u}{\delta X} & \frac{\delta u}{\delta Y} & \frac{\delta u}{\delta Z} \\ \frac{\delta u}{\delta X} & \frac{\delta u}{\delta Y} & \frac{\delta u}{\delta Z} \\ \frac{\delta u}{\delta X} & \frac{\delta u}{\delta Y} & \frac{\delta u}{\delta Z} \end{bmatrix} \tag{4}$$

The deformation gradient tensor F can show how an infinitesimal line element, $d\mathbf{X}$ is mapped to the corresponding deformed line element $d\mathbf{x}$ by

$$d\mathbf{x} = \frac{\delta \mathbf{x}}{\delta \mathbf{X}} d\mathbf{X} = F\, d\mathbf{X} \tag{5}$$

The deformation gradient $\mathbf{F}$ contains the complete information about the local straining and rotation of the material [25]. The deformation gradient $\mathbf{F}$, can also be written in terms of the displacement gradient as

$$d\mathbf{x} = \frac{\delta \mathbf{x}}{\delta \mathbf{X}} = \nabla \mathbf{u} + I \tag{6}$$

When a material stretches it will cause changes in the material density. The ratio between the current and the initial mass density is given by

$$\frac{dV}{dV_0} = \frac{\rho_0}{\rho} = det(F) = J \tag{7}$$

In Equation (7), ρ_0 is the initial density and ρ is the current density after deformation. The determinant of the deformation gradient tensor F is related to volumetric changes with respect to the initial state [25].

The mass density should be constant when using the material formulations used in the structural mechanics interface. This is because the equations

are formulated for fixed material particles. Therefore, temperature-dependent material date for the mass density should not be used. The changes in volume caused by temperature changes are incorporated using the coefficient of thermal expansion in the material model, when combined with the Thermal Expansion module [25].

2.2 Thermal Expansion

When there are temperature changes, most materials react by a change of volume. For a constrained structure, the stresses that evolve with even moderate temperature changes can be considerable. In COMSOL, the volume change is represented as a thermal strain ε_{th}, which produces stress-free deformations. For a linear elastic material, the constitutive law is [25]

$$s = s_0 + c : \varepsilon - \varepsilon_0 - \varepsilon_{th} \tag{8}$$

In the computations, the thermal expansion appears as a load, even though it formally is a part of the constitutive relations.

2.3 Joule Heating Interface

The Joule Heating interface is used to model resistive heating. The multiphysics interface combines the Electric Currents interface and the Heat Transfer in Solids interface. The couplings add the electromagnetic power dissipation as a heat source, and the electromagnetic material properties can depend on the temperature. The Electromagnetic Heat Source multiphysics coupling represents the source term $\mathbf{Q}_e$ $(SIunit : W/m^3)$ in the heat equation implemented by [26]

$$\rho C_p \frac{\delta T}{\delta t} - \nabla \cdot (k \nabla T) = \mathbf{Q}_e \tag{9}$$

The resistive heating (ohmic heating) due to the electric current is

$$\mathbf{Q}_e = \mathbf{J} \cdot \mathbf{E} \tag{10}$$

where $\mathbf{J}$ is the current density $(SI\ unit : A/m^2)$, and $\mathbf{E}$ is the electric field strength $(SI\ unit : V/m)$.

2.4 Heat Transfer

The fundamental law governing all heat transfer is the fist law of thermodynamics, which is commonly referred as the principle of conservation of energy. In COMSOL the law is rewritten in terms of the temperatur, $\mathbf{T}$. The resulting heat equation is [26]:

$$\rho C_p \left(\frac{\delta T}{\delta t} + (\mathbf{u} \cdot \nabla) T \right) + \nabla \cdot \mathbf{q} = \tau : \mathbf{S} - \frac{T}{\rho} \frac{\delta \rho}{\delta T} \bigg|_p \left(\frac{\delta p}{\delta t} + (\mathbf{u} \cdot \nabla) p \right) + Q \tag{11}$$

where

- ρ is the density $(SI\ unit : kg/m^3)$
- C_p is the specific heat capacity at constant pressure $(SI\ unit : J/(kg \cdot K))$
- T is the absolute temperature $(SI\ unit : K)$
- $\mathbf{u}$ is the velocity vector $(SI\ unit : m/s)$
- $\mathbf{q}$ is the heat flux by conduction $(SI\ unit : W/m^2)$
- p is the pressure $(SI\ unit : Pa)$
- $\mathbf{S}$ is the strain tensor $(SI\ unit : 1/s)$

3. Design and Simulation

In our simulation we first created a 3D model of the structure using COMSOL's modeling environment. Specific materials were selected and assigned to each domain, Table 1 show the properties of the materials used in our simulation.

Our design, has $10\,\mu m$ metal lines of gold under the bimorph beams, as shown in Fig. 2. The metal lines that run under the beam actuators are connected at its edges, to a thicker line that are routed under the buckled cantilevers to the contact pads.

When a voltage is applied, a current is passed through the metallization layer and this will act as the heating element of the actuators. The temperature will increase, and the metal layer (with a higher coefficient of thermal expansion) will have a larger deformation than the polyimide. Therefore, the bilayer structure will bend toward the polymer side.

Due to the small dimension of MEMS devices, direct measurement of their electrical and mechanical properties is a challenge [6]. The device

Table 1: Materials properties

Property	Polyimide	Gold
Coefficient of thermal expansion (α), $1/K$	$3*10^{-6}$	$14.2*10^{-6}$
Young's modulus (E), GPa	8.5	70
Poisson's ratio (ν)	0.34	0.44
Density (ρ), kg/m^3	1300	19300
Reference temperature (T), K	293	293
Reference resistivity (σ_r), Ωm	$1.5*10^17$	$2.44*10^{-8}$

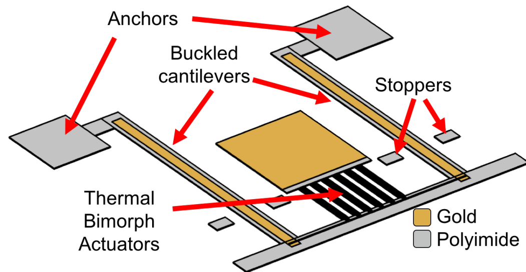

Figure 2: Bottom Isometric View of a BCP with integrated thermal bimorph actuators. The design has si bimorph actuator beams, with a width of $50\mu m$ and $10\mu m$ metal lines

is comprised of a compliant mechanism and several thin layers, which makes a complex system to model analytically. A way to tackle this problem, is by using numerical methods to do an approximation of the desired results.

To simulate the assembly of the structure we used the Solid Mechanics interface. The anchors features of the structure were set with a fixed constraint. The free end of the structure was set to have a prescribed displacement. With the help of an auxiliary sweep and setting the study for large deformations (include geometric nonlinearity option) we were able to simulate the assembly. A BCP conceptual assembly procedure is shown in Fig. 3

We used COMSOL to simulate the assembly process and then use the solution, to compute another study to solve the Joule Heating problem

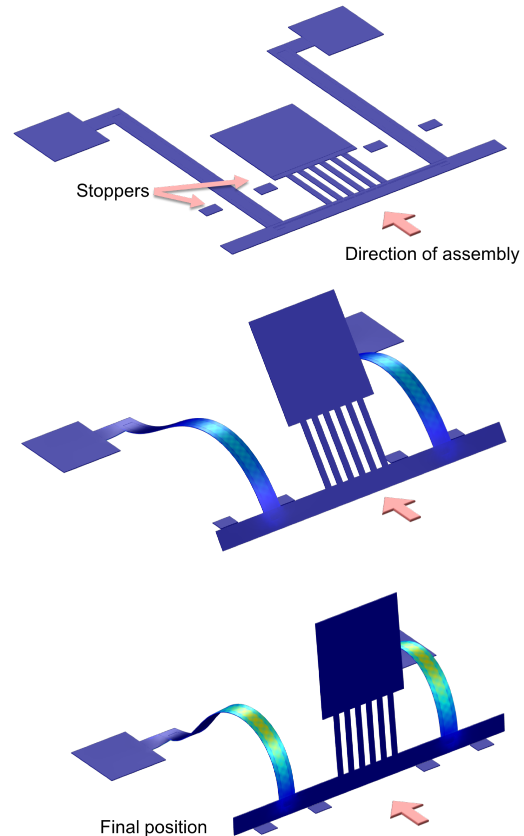

Figure 3: Buckled Cantilever Plate assembly sequence. The initial position of the structure after fabrication is flat (in-plane) on top of the silicon substrate. A microprobe is used to push the free end of the structure (depicted with the thick arrow). A set of stoppers are used to keep the device in its assembly position.

and thermal expansion. The solution was used as a dependent for the heat transfer simulation. The boundary conditions applicable to the second study are: the environment temperature, the heat flux dissipation and the potential applied to the metal boundary faces (one set as ground and the other one to an electric potential).

4. Results

Our main goal was to determine a reliable approximation of the behavior of our fabricated device, and to verify and optimize the device before its fabrication. The displacement assembly simula-

tion is shown in Fig. 3. The simulation results of both: assembled structure and the joule heating results are shown in Fig. 4.

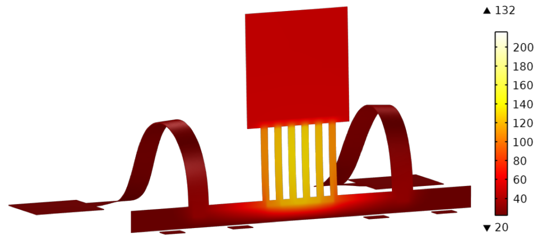

Figure 4: Scanning Electron Microscope (SEM) image of an assembled BCP structure with thermal bimorph actuators.

The results of the simulated device are in good agreement with the experimental measured temperature, see Fig. 5. In this experiment, we applied an operation voltage of $4V$, where the bimorph actuators reached a maximum temperature of $130\,^{\circ}C$. In both Fig. 4 and 5, it can be seen that the temperature generated in the bimorph actuators has a low impact on the plate's temperature. Therefore, other MEMS devices could be located on the plate, extending the possible device's applications.

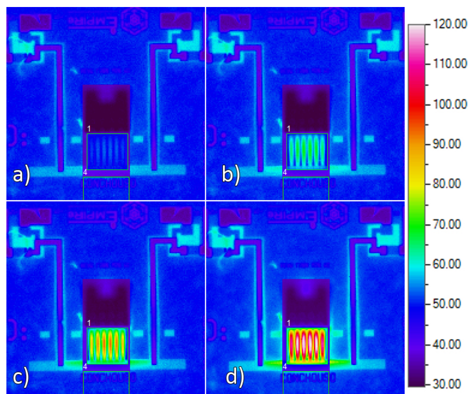

Figure 5: Optotherm InfraSight thermal image of the actuated BCP at different voltage levels [24].

The experimental displacement of the plate was compared to the simulation results of the thermal expansion study, in order to validate our model. The relative tip displacent for both experimental and simulated results are shown in Fig. 6. These results have excellent agreement, showing that there is a good approximation to the real device.

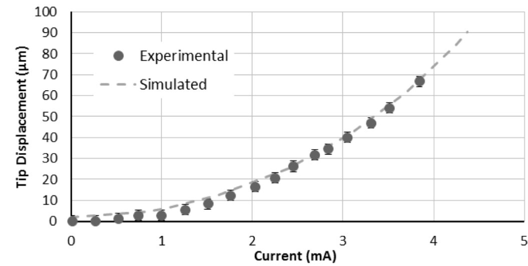

Figure 6: Simulation results and experimental measurements comparison [24].

In Fig. 7, a set of images show the fabricated devices mounted on its testing board. The chips are fabricated using the Polyimide-Metal-MEMS Process (PiMMP) [22]. Wafer is diced in $2.3\,cm$ by $2.3\,cm$, using a dicing saw or methods reported elsewhere [27].

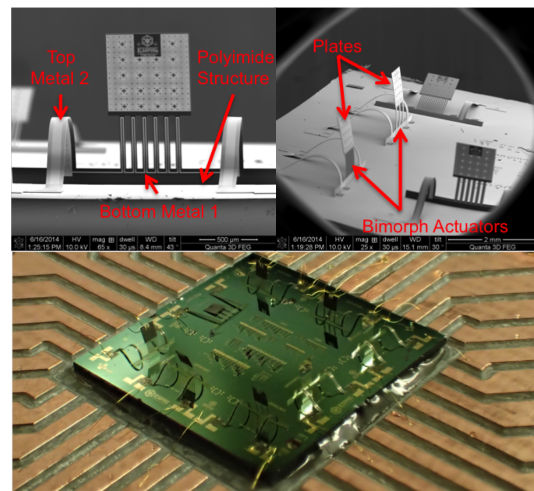

Figure 7: (Top) SEM images of the fabricated BCPs with thermal bimorph actuators. (Bottom) Optical image or the mounted fabricated chip on its testing board [3].

5. Conclusions

We have presented the simulation of BCP with integrated bimorph actuators, that can adjust the angle of the structural plate. The device has been fabricated with two metals: one under the polyimide layer and one on top. This allows a bidirectional control of the angle. The precision of the position of the plate is in the nanometer

range. Due to its characteristics, the structure could potentially be used in several MEMS applications that require thermal and electrical isolation from the substrate. The device could be potentially used in the development of a micro-optical bench, where the structures could help in the control of optical switches by blocking optical paths. Sweeping antennas and bar code scanners, could also benefit from this technology. Moreover, the validation and good agreement between the simulation and the experimental data, allow us to use the model to optimize and design better structures.

6. References

1. D Sameoto, A H Ma, M Parameswaran, and A M Leung. Assembly and Characterization of Buckled Cantilever Platforms for Thermal Isolation in a Polymer Micromachining Process. In *Electrical and Computer Engineering, 2007. CCECE 2007. Canadian Conference on*, pages 296–299, (2007).

2. A Arevalo, D Conchouso, E Rawashdeh, D Castro, and I G fould. Platform Isolation Using Out-of-Plane Compliant Mechanisms. In *2014 COMSOL Conference, Boston, USA* (2014).

3. D Conchouso, A Arevalo, D Castro, , and I G Foulds. Out-of-plane Platforms with Bidirectional Thermal Bimorph Actuation for Transducer Applications. In *10th IEEE International Conference on Nano/Micro Engineered and Molecular Systems NEMS2015*, Xia'an (2015).

4. Dan Sameoto, Ted Hubbard, and Marek Kujath. Operation of electrothermal and electrostatic MUMPs microactuators underwater. *Journal of Micromechanics and Microengineering*, **14**(10):1359–1366 (2004).

5. Armando Arpys Arevalo Carreno, David Conchouso, and Ian G Foulds. Optimized Cantilever-to-Anchor Configuration of Buckled Cantilever Plate Structures for Transducer Applications. In *2012 COMSOL Conference, Milan, Italy*, (2012).

6. D Castro, A Arevalo, E Rawashdeh, and N Dechev. Simulation of a Micro-Scale Out-of-plane Compliant Mechanism. In *2014 COMSOL Cambridge, England*, (2014).

7. See-Ho Tsang, D Sameoto, and M Parameswaran. Out-of-plane electrothermal actuators in silicon-on-insulator technology. *Electrical and Computer Engineering, Canadian Journal of*, **31**(2):97–103, (2006).

8. Loïc Marnat, A Arevalo Carreno, D Conchouso, M Galicia Martinez, I Foulds, and Atif Shamim. New Movable Plate for Efficient Millimeter Wave Vertical on-Chip Antenna. *IEEE Transactions on Antennas and Propagation*, **61**(4):1608–1615, (2013).

9. A Arevalo, E Byas, and I G Foulds. μHeater on a Buckled Cantilever Plate for Gas Sensor Applications. *2012 COMSOL Conference, Milan, Italy*, (2012).

10. Abdul Haseeb Ma and Albert M Leung. Three-axis thermal accelerometer based on buckled cantilever microstructure. pages 1492–1495, (2008).

11. A Alfadhel and Arpys Arevalo. Three-Axis Magnetic Field Induction Sensor Realized on Buckled Cantilever Plate. *IEEE Transactions in Magnetics*, **49**(7):4144–4147 (2013).

12. N Jaber, A Ramini, A Carreno, and MI Younis. Higher Order Modes Excitation of Micro Clamped-Clamped Beams. *NANOTECH Dubai 2015*, (2015).

13. A A A Carreno, D Conchouso, A Zaher, I Foulds, and J Kosel. Simulation of a Low Frequency Z-Axis SU-8 Accelerometer in CoventorWare and MEMS+. In *Computer Modelling and Simulation (UKSim), 2013 UKSim 15th International Conference on*, pages 792–797, (2013).

14. D Conchouso, A Arevalo, D Castro, E Rawashdeh, M Valencia, A Zaher, J Kosel, and I Foulds. Simulation of SU-8 Frequency-Driven Scratch Drive Actuators. In *Computer Modelling and Simulation (UKSim), 2013 UKSim 15th International Conference on*, pages 803–808, (2013).

15. J P Rojas, A Arevalo, I G Foulds, and M M Hussain. Design and characterization of ultra-stretchable monolithic silicon fabric. *Applied Physics Letters*, **105**(15):154101, (2014).

16. J P Rojas, Hussain A M, A Arevalo, I G Foulds, Sevilla GAT, JM Nassar, and M M Hussain. Transformational electronics are now reconfiguring. *SPIE Defense+ Security*, **9467**:946709–946709–7, (2015).

17. A Arevalo, S Ilyas, D Conchouso, and I G Foulds. Simulation of a Polyimide Based Micromirror. *2014 COMSOL Conference*, (2014).

18. A Arevalo and I G Foulds. Polyimide Thermal Micro Actuator. *2014 COMSOL Conference, Cambridge, England*, (2014).

19. Arpys Arevalo and I G Foulds. Parametric Study of Polyimide–Lead Zirconate Titanate Thin Film Cantilivers for Transducer Applications. *COMSOL Rotterdam*, (2013).

20. Saad Ilyas, Abdallah Ramini, and Mohammad I Younis. An Experimental and Theoretical Investigation of a Micromirror Under Mixed-Frequency Excitation. *Journal of Microelectromechanical Systems*, pages 1–1, ().

21. A Arevalo and I G Foulds. MEMS Acoustic Pixel. *2014 COMSOL Conference, Cambridge, England*, (2014).

22. A Arevalo, E Byas, D Conchouso, D Castro, S Ilyas, and I G Foulds. A Versatile Multi-User Polyimide Surface Micromachining Process for MEMS Applications. In *10th IEEE International Conference on Nano/Micro Engineered and Molecular Systems NEMS2015*, Xia'an (2015).

23. A Arevalo, D Conchouso, D Castro, N Jaber, M I Younis, and I G Foulds. Towards a Digital Sound Reconstruction MEMS Device: Characterization of a Single PZT Based Piezoelectric Actuator. In *10th IEEE International Conference on Nano/Micro Engineered and Molecular Systems NEMS2015*, Xia'an (2015).

24. A Arevalo, D Conchouso, D Castro, M Diaz, and I G Foulds. Out-of-plane buckled cantilever microstructures with adjustable angular positions using thermal bimorph actuation for transducer applications. *Micro and Nano Letters*, (2015).

25. COMSOL Multiphysics. Structural mechanics module user's guide. (2015).

26. COMOSL. Comsol multiphysics reference manual. (2015).

27. Y Fan, A Arevalo, H Li, and I G Foulds. Low-cost silicon wafer dicing using a craft cutter. *Microsystem Technologies*, (2014).